Optimal Sensor Placement for Acoustic Range-Based Underwater Robot Positioning

Thomas Glotzbach*. David Moreno-Salinas.**
Antonio Pascoal*. Joaquin Aranda ****

** Institute for Automation and Systems Engineering, Ilmenau University of Technology, Ilmenau, Germany (Tel: +49-3677-69-4107; e-mail: thomas.glotzbach@tu-ilmenau.de).*
*** Departamento de Informática y Automática, ETSI Informática, Universidad Nacional de Educación a Distancia (UNED), Madrid, Spain (e-mail: {dmoreno,jaranda}@dia.uned.es)*
**** Laboratory of Robotics and Systems in Engineering and Science (LARSyS), Instituto Superior Técnico (IST), Univ. Lisbon, Portugal; Adjunct Scientist, National Institute of Oceanography (NIO), Goa, India (e-mail: antonio@isr.ist.utl.pt)}*

Abstract: This paper addresses the problem of optimal sensor placement for acoustic range-based underwater target positioning. In particular, we focus on the experimental set-up whereby target positioning is performed by measuring the ranges between the underwater target and a number of surface units equipped with acoustic ranging devices and GPS. With the objective of affording the reader a concise overview of the main theoretical challenges involved, this paper starts with a survey of previous work done in the area, including that of the authors. By casting the problem at hand in the form of a classical estimation problem we describe and solve the equivalent mathematical problem of maximizing the determinant of a conveniently defined Fisher Information Matrix (FIM). The latter is related to the Cramér-Rao Bound, which equals the smallest possible position estimation error variance that can possibly be achieved with any unbiased estimator. To further clarify the presentation, the details of Monte Carlo simulations in 2D and 3D with a selected target positioning algorithm are included to confirm the theoretical results numerically.

Keywords: Autonomous Underwater Vehicles, Underwater Navigation, Optimal Sensor Placement, Fisher Information Matrix, Cramér-Rao Bound, Maximum Likelihood Estimation

1. INTRODUCTION

Navigation plays a key role in marine robotics and is currently the subject of intensive research worldwide, especially in underwater scenarios. In the latter type of missions, autonomous marine vehicles must travel over large distances to acquire scientific ocean data at unprecedented scales, while being able to geo-reference the data acquired by resorting to advanced navigation systems. Navigation, in this context, refers to the task of estimating the position of a vehicle underwater. Submerged vehicles have no access to absolute navigation data. In many operational scenarios the only navigation data accessible are those acquired by on-board resident sensor units. Affordable, classical navigation systems that rely solely on these data will necessarily exhibit errors that grow with time, and must be complemented with external aids. The latter may include acoustic systems capable of estimating the position of the vehicle with respect to a set of transponders. In what follow, we give a very brief overview of range-based positioning systems.

To estimate the position of an underwater agent by means of acoustic range measurements, one needs several objects (*reference objects* or *ROs* henceforward) equipped with sensors capable of measuring these ranges and determining their own position with high precision. A possible solution is to place the ROs at the surface and use GPS to locate them. A system that employs surface buoys as ROs in order to estimate the position of an underwater object is referred to as GIB (GPS Intelligent Buoys). A modification of the commercially available system that relies on the use of an Extended Kalman Filter (EKF) is described in detail in Alcocer, Oliveira, and Pascoal (2007). The key ideas behind the GIB concept were exploited and extended in Glotzbach et al. (2012) to develop a system capable of estimating the position of a human diver, and where no time synchronization is required between the target and the ROs (as is the case with the original GIB system). Also, small unmanned surface crafts were employed as ROs. This fact gave rise to another interesting problem, namely that of correct placement of the companion surface vehicles. This task is referred to as Optimal Sensor Placement (OSP) and can be cast in the form of an Estimation Theoretical Problem that involves the computation of the Cramér-Rao-Bounds to compute the best positioning performance that can be achieved with any unbiased position estimator. Naturally, the optimal placement solution is a function of the actual measurement setup, the measurement model, and the actual position of the target.

At first inspection this problem may seem to have little practical relevance, for it could be argued that if the target position were known in advance, then the need to locate it would not arise. This argument can be countered by stating that, firstly, this research aims to provide a general

understanding of the dependence between target position and optimal acoustic sensor positions. For real sea operations, where the accuracy of range measuring devices is plagued by intermittent failures, outliers, and multipath propagation effects, it is important to have an understanding of the best sensor geometry in idealized situations. Secondly, localization under real conditions may end up being an iterative process. In this case, it is reasonable to get a first, possibly "rough" estimate of the target position, and then use this position to perform Optimal Sensor Placement. Once the sensors are placed in a new optimal configuration, the position of the target can be re-computed and the positioning/estimation cycle continues. Thirdly, to track a moving target over a large area, the ROs *have* to move alongside with the target. In this case, again it seems reasonable to organize their movement in an optimal way with respect to the current position estimate of the target, instead of simply letting them move "roughly" in the same direction as the target. Finally, the circle of ideas exploited in this paper may be extended to deal with the situation where prior information about the actual target position is available (e.g. in terms of a probability density function, as done by Isaacs, Klein, and Hespanha (2009)).

This paper should be viewed in part as a survey paper of work done in this area, and as such it borrows considerably from work done by the authors, see Moreno-Salinas et al. (2010), Moreno-Salinas et. al (2011), and the references therein. However, it goes one step further in that it includes not only results on optimal sensor placement, but also on Monte Carlos simulations with a selected target positioning algorithm aimed at confirming the theoretical results described. The work summarized here and in the two mentioned publications sought inspiration from the work of Martínez and Bullo (2006) on Optimal Sensor Placement for range-based localization of ground robots, where the authors placed the emphasis on the task of finding the optimal sensor positions for the acoustic ranging devices, the latter being allowed to move in a convex domain around the area in which the target is known to lie.

In contrast with the work in Martínez and Bullo (2006), we seek to characterize explicitly for both the 2D and 3D cases the optimal sensor positions in terms of their distances to the target to be located. The results are validated through Monte Carlo Simulations using MATLAB.

2. PROBLEM DESCRIPTION AND BRIEF LITERATURE SURVEY

Consider a stationary underwater target located at position $q_0=[x_0\ y_0\ z_0]^T$ and a number of Reference Objects (ROs) at the surface, capable of measuring the ranges to the target. As discussed above, we assume that the position of the target is known in advance in order to find the optimal location of the ROs (acoustic sensors). For the sake of simplicity, we assume that $x_0 = y_0 = 0$, that is, the target is located at the origin of the coordinate system for a 2D-scenario or at the depth coordinate z_0 below the origin for a 3D-scenario. We further assume there are n Reference Objects (ROs). Let $p_i \in \Re^m$;

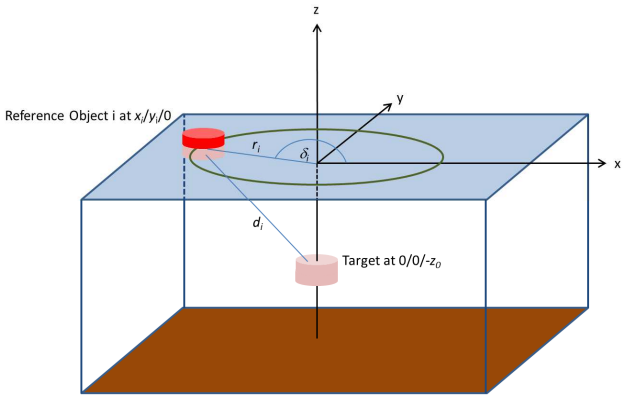

Fig. 1: Positioning system – Set-up and parameter description for the 3D case (only one RO is shown).

$i \in \{1,...,n\}$ be the position of the i^{th} RO, where m is equal to *2* or 3, for the 2D and 3D scenarios, respectively. Further let

$$z_i(q) = h(\|q - p_i\|) + w_i \tag{1}$$

be the measurement (obtained at the ith RO) of the distance between its position p_i and the target at position q. Here, the function h yields the actual distance between the target and each of the ROs, as long as it remains in the measurable range of the employed acoustic modems, that is,

$$h(\|q - p_i\|) = d_i = \begin{cases} r_i = \sqrt{x_i^2 + y_i^2} & \text{for 2D} \\ \sqrt{r_i^2 + z_0^2} = \sqrt{x_i^2 + y_i^2 + z_0^2} & \text{for 3D} \end{cases}, \tag{2}$$

Note that r_i is also the range-coordinate of the reference object in a 2D polar coordinate system which will be used later. In the 2D case, r_i equals d_i and will be used instead, see Fig. 1. We further introduce the column vector **H**, which contains the n ranges between the target and the ROs.

The term w_i in eq. (1) represents a zero mean white noise Gaussian process with variance σ^2. We also define the vector **Z** that contains the measurement values of all ROs:

$$\mathbf{Z} \triangleq \begin{bmatrix} z_1 \\ \vdots \\ z_n \end{bmatrix} \sim \mathbf{N}\left(\begin{bmatrix} h(\|q - p_1\|) \\ \vdots \\ h(\|q - p_n\|) \end{bmatrix}, \mathbf{R} \right), \tag{3}$$

where **R** is the covariance matrix, $\mathbf{R} = \sigma^2 \mathbf{I}_n$.

Equipped with the above definitions, we now seek to find the spatial configuration for the ROs that is optimal in a well defined sense. We will assume that the ROs will be placed at a circle with radius r, with r as the parameter to optimize. The rationale for this computational procedure is firmly rooted in estimation theory and was described in a vey elegant manner in Martínez and Bullo (2006) for the case of optimal sensor placement for range-based positioning of wheeled robots in 2D. In their work, the authors derived the optimal angular distribution between the ROs that maximizes the determinant of the Fisher Information Matrix (FIM) associated with the particular estimation problem at hand. The latter, as is well known, yields (after computing the related Cramer-Rao-Bound), relevant information on the best possible performance in target positioning that can possibly be achieved with any unbiased estimator, where performance is evaluated in terms of the variance of the position estimates.

See for example Taylor (1979) and van Trees (2001) as well as Porat and Nehorai (1996) and Ucinski (2004) for lucid presentations of the above topics.

3. OPTIMAL SENSOR PLACEMENT (ANALYTICAL COMPUTATIONS)

Following classical estimation theory, the Fisher Information Matrix (FIM) (denoted as J_{NR} for non-random parameters), corresponding to the problem of estimating the target position q based on measurements $\mathbf{Z}$, can be computed from the likelihood function Λ to yield

$$J_{NR} \triangleq E\left[\left(\nabla_q \log \Lambda\right)\cdot\left(\nabla_q \log \Lambda\right)^T\right] \tag{4}$$

where

$$\Lambda = \frac{1}{\sqrt{2\cdot\pi\cdot\det R}}\exp\left(-\frac{1}{2}(Z-H)^T R^{-1}(Z-H)\right). \tag{5}$$

Taking the logarithm of (5), calculating the gradient with respect to q, and introducing c as a combination of all parameters that do not depend on q), one obtains:

$$\nabla_q \log \Lambda = \nabla_q\left[c-\frac{1}{2}(Z-H)^T R^{-1}(Z-H)\right] = \nabla_q H^T\cdot R^{-1}(Z-H). \tag{6}$$

Inserting (6) in (4), straightforward computations (see for example Alcocer (2009)) imply that

$$J_{NR} = \nabla_q H^T\cdot R^{-1}\cdot\nabla_q H\,. \tag{7}$$

Following the definitions and computations in Martínez and Bullo (2006), we define

$$\partial_l h_i(q_0, p_1,..., p_n) \triangleq \frac{\partial}{\partial q^l} h\left(\left\|q-p_i\right\|\right)\Big|_{q=q_0}, \tag{8}$$

for $i\in\{1,...,n\}$ and $l\in\{1,...,m\}$.

It then follows from above that

$$\begin{aligned} J_{NR} &= \frac{1}{\sigma^2}\left(\nabla_q H\right)^T_{q_0}\left(\nabla_q H\right)_{q_0} \\ &= \frac{1}{\sigma^2}\sum_{i=1}^{n}\begin{bmatrix}(\partial_1 h_i)^2 & \cdots & (\partial_1 h_i)(\partial_d h_i)\\ \vdots & \ddots & \vdots \\ (\partial_d h_i)(\partial_1 h_i) & \cdots & (\partial_d h_i)^2\end{bmatrix}. \end{aligned} \tag{9}$$

From the discussions in the previous Section, the problem of optimal sensor placement is equivalent to that of computing

$$(p_1,..., p_n) = \arg\max \mathcal{L}_{q_0}(p_1,..., p_n). \tag{10}$$

where the cost function $\mathcal{L}_{q0}$ is defined as

$$\mathcal{L}_{q_0}(p_1,..., p_n) = \det J_{NR}(q_0, p_1,..., p_n) \tag{11}$$

After inserting (9) in (10) it can be shown, using the techniques described in Martínez and Bullo (2006) and Aranda et al. (2004) that the above cost function can be expressed for the 2D case as

$$\mathcal{L}_{q_0} = \frac{1}{2\sigma^2}\sum_{i,j=1}^{n}\|v_i\|^2\|v_j\|^2\sin^2\alpha_{ij} \tag{12}$$

with $v_i = [\partial_1 h_i \quad \partial_2 h_i \quad 0]^T$, $\alpha_{ij} = \angle(v_i, v_j)$,

and for the 3D case as

$$\mathcal{L}_{q_0} = \frac{1}{6\sigma^2}\sum_{i,j,k=1}^{n}\|v_i\|^2\|v_j\|^2\|v_k\|^2\sin^2\alpha_{ij}\cos^2\beta_{ij,k} \tag{13}$$

with $v_i = [\partial_1 h_i \quad \partial_2 h_i \quad \partial_3 h_i]^T$, $\alpha_{ij} = \angle(v_i, v_j)$, $\beta_{ij,k} = \angle(v_i\times v_j, v_k)$.

We now describe the most important results on optimal sensor placement.

3.1 2D Case

We start by adapting (12) to the scenario described in Section 2. Equation (2) implies that

$$\partial_1 h_i = \frac{\partial}{\partial x}\sqrt{x_i^2+y_i^2} = \frac{x_i}{r_i}\,. \tag{14}$$

Similarly for $\partial_2 h_i$, we obtain

$$\|v_i\|^2 = (x_i/r_i)^2 + (y_i/r_i)^2 = x_i^2+y_i^2/r_i^2 = 1\,. \tag{15}$$

Let α_{ij} be the angle between v_i and v_j. Using the definition of the scalar product, it follows that

$$v_i\cdot v_j = \|v_i\|\cdot\|v_j\|\cdot\cos\alpha_{ij} \Rightarrow \alpha_{ij} = \arccos\left[\left(x_i x_j + y_i y_j\right)/r_i r_j\right]. \tag{16}$$

Furthermore, inserting (15) and (16) in (12) yields

$$\mathcal{L}_{q_0} = \frac{1}{2\sigma^2}\sum_{i,j=1}^{n}\sin^2\left(\arccos\frac{x_i x_j + y_i y_j}{r_i r_j}\right). \tag{17}$$

From the fact that $\sin(\arccos(\alpha)) = \sqrt{1-\alpha^2}$, it follows after lengthy computations that

$$\mathcal{L}_{q_0} = \frac{1}{2\sigma^2}\sum_{i,j=1}^{n}\frac{\left(x_i y_j - x_j y_i\right)^2}{r_i^2 r_j^2}\,. \tag{18}$$

In preparation for the computation of the optimal sensor locations we express their coordinates in polar form. With these coordinates, p_i is defined by distance r_i and angle δ_i, that is, $x_i = r_i\cos\delta_i$, $y_i = r_i\sin\delta_i$. Because $\sin\alpha\cos\beta - \sin\beta\cos\alpha = \sin(\alpha-\beta)$, $\mathcal{L}_{q0}$ can be written as

$$\begin{aligned}\mathcal{L}_{q_0} &= \frac{1}{2\sigma^2}\sum_{i,j=1}^{n}\frac{\left(r_i\cos\delta_i r_j\sin\delta_j - r_j\cos\delta_j r_i\sin\delta_i\right)^2}{r_i^2 r_j^2} \\ &= \frac{1}{2\sigma^2}\sum_{i,j=1}^{n}\frac{r_i^2 r_j^2\left(\cos\delta_i\sin\delta_j - \cos\delta_j\sin\delta_i\right)^2}{r_i^2 r_j^2} = \frac{1}{2\sigma^2}\sum_{i,j=1}^{n}\sin^2\left(\delta_i-\delta_j\right)\end{aligned}. \tag{19}$$

From the above expression two conclusions can be drawn: i) the value of the determinant of the Fisher Information Matrix does not depend on the ranges of the sensors in a 2D scenario, and ii) the determinant depends only on the angles of the sensors in a polar coordinate system; namely, on the differences between those angles. The reader will find in Martínez and Bullo (2006) a proof that the optimal sensor

placement corresponds to having the sensors placed symmetrically in a circumference around the target position

3.2 3D Case

We use a procedure similar to that discussed in Section 3.1 to tackle the 3D case. Expressions (14) and (15) are easily generalized by replacing r_i with d_i, for the target depth z_0 must now be considered. From the fact that

$$\partial_3 h_i = \frac{\partial}{\partial z}\sqrt{x_i^2 + y_i^2 + z_0^2} = \frac{z_0}{d_i}. \quad (20)$$

and the constraint that the norm of v_i equals 1, it follows that

$$\mathcal{L}_{q_0} = \frac{1}{6\sigma^2}\sum_{i,j,k=1}^{n} \sin^2\alpha_{ij}\cos^2\beta_{ij,k} \quad (21)$$

We now derive different expression for the sin- and the cos-factors above. For the sin-factor we can easily adapt the result in(16) to obtain

$$\alpha_{ij} = \arccos\left[\left(x_i x_j + y_i y_j + z_0^2\right)/d_i d_j\right]. \quad (22)$$

Computations similar to those involved in going from (17) to (18) allow us to write

$$\begin{aligned}\sin^2\alpha_{ij} &= \sin^2\left(\arccos\frac{x_i x_j + y_i y_j + z_0^2}{d_i d_j}\right). \\ &= 1 - \frac{\left(\left(x_i x_j + y_i y_j\right) + z_0^2\right)^2}{\left(x_i^2 + y_i^2 + z_0^2\right)\left(x_j^2 + y_j^2 + z_0^2\right)}\end{aligned} \quad (23)$$

It is now possible to show that the above equation degenerates into

$$\sin^2\alpha_{ij} = \frac{\left\{\left(x_j y_i - x_i y_y\right)^2 + \left(x_i z_0 - x_j z_0\right)^2 + \left(y_i z_0 - y_j z_0\right)^2\right\}}{d_i^2 d_j^2}. \quad (24)$$

For the cos- factor in (21), $\beta_{ij,k}$ is the angle between the cross product (v_i x v_j) and v_k. From the definition of the scalar product, it follows that

$$\begin{aligned}&\left(v_i \times v_j\right)\cdot v_k = \left\|v_i \times v_j\right\|\cdot\|v_k\|\cdot\cos\beta_{ij,k} \\ &\Rightarrow \cos^2\beta_{ij,k} = \left(\frac{\left(v_i \times v_j\right)\cdot v_k}{\left\|v_i \times v_j\right\|}\right)^2\end{aligned}. \quad (25)$$

Because the above cross product equals

$$v_i \times v_j = \left(\frac{y_i z_0 - y_j z_0}{d_i d_j} \quad \frac{x_j z_0 - x_i z_0}{d_i d_j} \quad \frac{x_i y_j - x_j y_i}{d_i d_j}\right)^T, \quad (26)$$

the numerator in the expression on the right side of (25) can be computed as

$$\begin{aligned}\left[\left(v_i \times v_j\right)v_k\right]^2 &= \left(\frac{\left(y_i z - y_j z\right)x_k}{d_i d_j d_k} + \frac{\left(x_j z - x_i z\right)y_k}{d_i d_j d_k} + \frac{\left(x_i y_j - x_j y_i\right)z_0}{d_i d_j d_k}\right)^2, \\ &= z^2\frac{\left(x_k y_i - x_k y_j + x_j y_k - x_i y_k + x_i y_j - x_j y_i\right)^2}{\left\{d_i^2 d_j^2\right\}d_k^2}\end{aligned} \quad (27)$$

while the denominator equals

$$\left\|v_i \times v_j\right\|^2 = \frac{\left(y_i z_0 - y_j z_0\right)^2 + \left(x_j z_0 - x_i z_0\right)^2 + \left(x_i y_j - x_j y_i\right)^2}{\left\{d_i^2 d_j^2\right\}}. \quad (28)$$

Dividing equation (27) by (28), the terms in curly brackets are reduced. In the numerator of (28), the signs of the elements in the curved brackets can be changed, yielding

$$\cos^2\beta_{ij,k} = \frac{z_0^2\left(x_k y_i - x_k y_j + x_j y_k - x_i y_k + x_i y_j - x_j y_i\right)^2}{d_k^2\left\{\left(y_j z_0 - y_i z_0\right)^2 + \left(x_i z_0 - x_j z_0\right)^2 + \left(x_j y_i - x_i y_j\right)^2\right\}}. \quad (29)$$

Finally, we use (24) and (29) in (21), which eliminates the terms in curly brackets, thus obtaining

$$\mathcal{L}_{q_0} = \frac{1}{6\sigma^2}\sum_{i,j,k=1}^{n}\frac{z_0^2\left(x_k y_i - x_k y_j + x_j y_k - x_i y_k + x_i y_j - x_j y_i\right)^2}{d_i^2 d_j^2 d_k^2}. \quad (30)$$

We are now interested in computing the optimal range for the ROs. We do this again in the 2D polar coordinate system, as the reference objects are surface vehicles. By assuming that the ranges are the same for all vehicles, using r as common range and d as common distance (see Fig. 1), yields

$$\mathcal{L}_{q_0} = \frac{1}{6\sigma^2}\sum_{i,j,k=1}^{n}\frac{z_0^2 r^4}{d^6}\left(\begin{array}{l}\cos\delta_k\sin\delta_i - \cos\delta_k\sin\delta_j + \cos\delta_j\sin\delta_k\cdots \\ \quad\cdots - \cos\delta_i\sin\delta_k + \cos\delta_i\sin\delta_j - \cos\delta_j\sin\delta_i\end{array}\right)^2. \quad (31)$$

We now replace d with (2), sort the terms to separate r- and non-r-dependent ones, and introduce a parameter c that contains all terms that are constant with respect to r:

$$\mathcal{L}_{q_0} = \frac{r^4}{\left(r^2 + z_0^2\right)^3}\cdot c \quad (32)$$

We now search for that r that maximizes (32). To this effect, we compute its gradient and set the result to 0, that is,

$$\begin{aligned}&\frac{\partial}{\partial r}\mathcal{L}_{q_0} = \frac{\partial}{\partial r}\frac{c\cdot r^4}{\left(r^2 + z_0^2\right)^3} = \frac{\partial}{\partial r}\frac{u}{v} = \frac{u'v - uv'}{v^2} \overset{!}{=} 0, \\ &u = cr^4,\ \ u' = 4cr^3,\ \ v = \left(r^2 + z_0^2\right)^3,\ \ v' = 3\cdot\left(r^2 + z_0^2\right)^2\cdot 2\cdot r\end{aligned}. \quad (33)$$

From the above, considering only the numerator gives

$$4cr^3\left(r^2 + z_0^2\right)^3 - cr^4\cdot 3\cdot\left(r^2 + z_0^2\right)^2\cdot 2\cdot r \overset{!}{=} 0. \quad (34)$$

Condition (34) is fulfilled for either r or c equal 0. These solutions are not feasible and will therefore be discarded. To characterize the other solutions divide (34) by $4\left(r^2 + z_0^2\right)^2$, which is greater than 0 for r greater than 0, to obtain

$$r^2 + z_0^2 - 1.5r^2 \overset{!}{=} 0 \quad (35)$$

$$0{,}5r^2 \overset{!}{=} z_0^2 \Rightarrow r \overset{!}{=} \sqrt{2}z_0 \text{ for } r \text{ greater than 0.} \quad (36)$$

We can conclude that the function of the determinant of the Fisher Information Matrix, written as a function of r, has critical points at 0, $\sqrt{2}\cdot z_0$ and $-\sqrt{2}\cdot z_0$. Fig. 2 shows a plot of the values of the determinant of the Fisher Information Matrix calculated for a 3D scenario with three ROs, z_0 = 10 m; and σ^2=1 m^2, as a function of the common distance r from the ROs to the origin. The plot is an interpolation of a number of points (identified by marks), computed by using (10). As predicted, the maximum value of the determinant is obtained for $r = \sqrt{2}z_0 = 14.142\,\text{m}$. Therefore, the radius of the

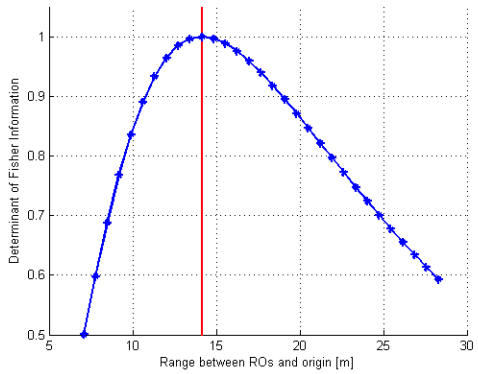

Fig. 2: Determinant of Fisher Information as function of common range r of the ROs.

sensor formation becomes larger as the depth of the target increases.

4. NUMERICAL VERIFICATION

4.1 Simulation Environment

For simulation purposes we assume a situation similar to that described in Section 3 and adopt the definitions made there. Three Reference Objects ($\mathbf{p_1}$, $\mathbf{p_2}$, $\mathbf{p_3}$) are placed at the surface (z_i=0 for 3D), with uniformly spatially distributed angular distances between them and identical ranges r_0, yielding the following coordinates in a polar coordinate system:

$$\mathbf{p}_i^p(t_k) = [r_0(t_k) \quad \delta_i(t_k) \quad 0]^T \tag{37}$$

with $\delta_i = \frac{2\pi(i-1)}{3}, \quad i \in \{1,2,3\}$

The Reference Objects can measure their distances to the target, disturbed by white noise with the variance σ^2= 0.1 m². For both 2D and 3D situations, we will perform five simulation runs. In each run, different values for r_0 are used which are located around the optimal value according to the discussions in Section 3, and for each different value of r_0, several virtual measurements are created. In each simulation we estimate the position of the target using the method of Maximum Likelihood with Ranges (ML-R) described in Alcocer (2009), which is an iterative descent algorithm, providing results very close to the Cramér-Rao Bound in optimal case. It is important to mention that in the scenarios considered with 3 ROs in one plane and one target at a defined depth, any method employed will have two optimal solutions: one at the correct target depth, the other one directly opposite with a negative depth ('fake' target above the surface). However, by appropriately choosing a starting position for the iterative algorithm below the surface, the algorithm will converge to the correct solution.

4.2 The Maximum Likelihood with Ranges (ML-R) Algorithm

Assume the target is at position $\mathbf{x}_{ML}=[x' \; y' \; z']^T$. Then, the distances between the target and the Reference Objects are given by

$$\mathbf{X} = \begin{bmatrix} \|x_{ML} - p_1\| \\ \vdots \\ \|x_{ML} - p_3\| \end{bmatrix} = \begin{bmatrix} \sqrt{(x'-x_1)^2 - (y'-y_1)^2 + z'^2} \\ \vdots \\ \sqrt{(x'-x_3)^2 - (y'-y_3)^2 + z'^2} \end{bmatrix}. \tag{38}$$

We now search for those values of $\mathbf{x}_{ML}$ (referred to as $\hat{p}_{ML-R}$) that maximize $p(\mathbf{Z}|\mathbf{X})$, that is, the probability of observing the actual measurements $\mathbf{Z}$, conditioned on $\mathbf{X}$. As is customary in estimation theory, the above probability is referred to as the likelihood function Λ, see (5). In practice, it is common to work with the log-likelihood function, introduced in (6), that consists of a parameter which is independent from the target position (denoted as c in (6)) and a second term that is subtracted from c. Therefore, it can be stated that maximizing $p(\mathbf{Z}|\mathbf{X})$ is equivalent to minimizing the second term of the log-likelihood function as shown in (6), which leads to the problem of computing

$$\hat{p}_{ML-R} = \arg\min\left(\frac{1}{2}(\mathbf{Z}-\mathbf{X})^T \mathbf{R}^{-1}(\mathbf{Z}-\mathbf{X})\right). \tag{39}$$

This problem can now be solved by using any iterative optimization algorithms. See for example Alcocer (2009) for the use of a Newton method employing the Armijo that we adopted in the present work.

4.3 Results of Simulations

For all simulations, we used the following procedure: Five simulation runs were performed. For the 2D case, each run consisted of 12 simulations, starting with r_0 = 5 m and ending with 500 m. In the 3D case, the values for r_0 were chosen in the interval from 5 m to 20 m. In each single simulation, 10,000 estimations were performed. That means, 10,000 different measurement value vectors with noise, $\mathbf{Z}$, have been created and were stored in a 'central' matrix. Within the same run, the same measurement vector was used for each simulation. For each of the simulation, estimations using the ML-R approach have been performed, always with the initial positions

$$\mathbf{x_a} = \left[\frac{x_1+x_2}{2} \quad \frac{y_1+y_2}{2}\right] \vee \left[\frac{x_1+x_2}{2} \quad \frac{y_1+y_2}{2} \quad \frac{z_0}{2}\right], \tag{40}$$

for the 2D and 3D cases, respectively. For the Armijo Rule, the values used were ε=10^{-5}, k_{max}=50, s=1, β=0.5, and σ=0.1, according to the definition in Alcocer (2009).

For the 2D scenario, the discussions in Section 3 led to the conclusion that the range r_0 of the Reference Objects has no influence on the quality of the estimation. To prove this result, the values used for r_0 covered the ranges from 5 m to 500 m. It can be verified that the variance of the estimation error is independent of the rage r_0, see Fig. 3. A small increase is visible for small ranges. The increase is within 1% of the overall value and results from small numerical errors.

For the 3D scenario, the discussions in Section 3 allowed us to conclude that the optimal range r_0 of the Reference Objects should be the square root of twice the depth of the target. As

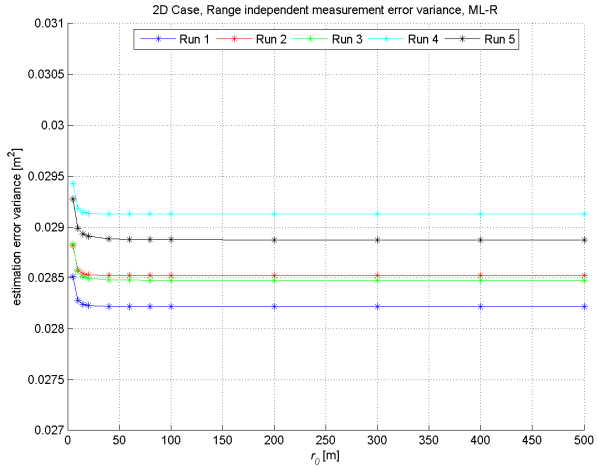

Fig. 3: Estimation Error Variance for the 2D case

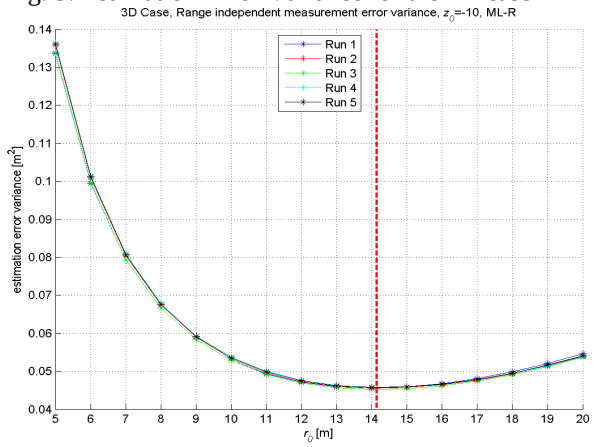

Fig. 4: Estimation Error Variance for the 3D case

the target is at a depth of 10 m, a range of 14.1 m should yield the best result for the estimation error variance. To prove this result, five simulation runs have been performed to cover the ranges from 5 m to 20 m. The results are displayed in Fig. 4. It can be observed that the minimum of the variance is exactly at the predicted range.

5. CONCLUSIONS

The work described in this paper is a contribution to the area of Optimal Sensor Placement for the localization of underwater targets in realistic marine scenarios. The paper started by affording the reviewer an overview of relevant principles, methods, and results available in the literature in the area, as well as of the practical motivation for this challenging topic of research. After a brief literature survey, a method was described to solve the problem of optimal sensor placement for range-based target positioning in 2D and 3D environments. In the latter case the target is submerged and the sensors are at the surface. The theoretical results derived were confirmed by means of Monte Carlo Simulations. Namely, it was confirmed in the 2D case, where the sensors are located on a circumference centered at the target and uniformly distributed along it, that the radius of he circumference does not have any influence on the accuracy of the target estimation. In contrast, in the 3D case the optimal range is a function of the target depth. Future work will address the problem of optimal sensor placement for single and multiple non-stationary target positioning, as well as transitioning from the laboratory to the real world.

ACKNOWLEDGMENTS

This research was supported in part by the Marie Curie Intra European Fellowship 'CONMAR' (N° 255216) and the Collaborative EC Project 'MORPH' (N° 288704), both funded by the 7th European Community Framework Programme. The work of the second and fourth author was partially supported by project DPI2009-14552-C02-02 of the Spanish Ministry of Science and Innovation.

REFERENCES

Aranda, S., Martínez, S., and Bullo, F. (2004). On optimal sensor placement and motion coordination for target tracking. *Technical Report CCEC-04-1013, CCDC*, University of California at Santa Barbara.

Alcocer, A., Oliveira, P., Pascoal, A. (2007). Study and implementation of an EKF GIB-based underwater positioning system. Control Engineering Practice Volume 15, Issue 6, pp. 689–701, Elsevier, 2007

Alcocer, A. (2009). Positioning and Navigation Systems for Robotic Underwater Vehicles, *Dissertation thesis of Instituto Superior Técnico*, Lisbon, Portugal, 2009

Glotzbach, Th., Bayat, M., Aguiar, A. P., Pascoal, A. (2012). An Underwater Acoustic Localisation System for Assisted Human Diving Operations. *9th IFAC Conference on Manoeuvring and Control of Marine Craft (MCMC), 2012*, Arenzano, Italy, no pagination.

Isaacs, J.T., Klein, D.J., and Hespanha, J.P. (2009). Optimal Sensor Placement For Time Difference of Arrival Localization, *Conference on Decision and Control, 2009* held jointly with the *2009 28th Chinese Control Conference (CDC/CCC 2009)*, pp. 7878-7884

Martínez, S., Bullo, F. (2006). Optimal sensor placement and motion coordination for target tracking, *Automatica 42*, p. 661 – 668.

Moreno-Salinas, D; Pascoal, A. M.; Alcocer, A; Aranda, J. (2010). Optimal Sensor Placement for Underwater Target Positioning with Noisy Range Measurements, 8th IFAC Conference on Control Applications in Marine Systems (CAMS 2010), Rostock, Germany.

Moreno-Salinas, D; Pascoal, A. M.; Aranda, J. (2011) Optimal Sensor Placement for Underwater Positioning with Uncertainty in the Target Location, 2011 IEEE International Conference on Robotics and Automation (ICRA 2011), pp. 2308 – 2314, Shanghai, China.

Porat, B., Nehorai, A. (1996). Localizing vapor-emitting sources by moving sensors. *IEEE Transactions on Signal Processing, 44(4)*, pp. 1018–1021.

Taylor, J.H. (1979), The Cramér-Rao Estimation Error Lower Bound Computation for Deterministic Nonlinear Systems, *IEEE Transactions on Automatic Control, Vol. AC-24, No. 2*, 1979

Ucinski, D. (2004). Optimal measurement methods for distributed parameter system identification. Boca Raton, FL: *CRC Press*, ISBN 0849323134

Van Trees, H.L. (2001). Detection, Estimation, and Linear Modulation Theory. *John Wiley & Sons Inc.*, New York, 2001